*33rd EPS Conference on Plasma Phys. Rome, 19 - 23 June 2006 ECA Vol.**30I**, P-5.009 (2006)*

Propagation velocity of relativistic electron beam in gas

B. K. Frolov, and S. I. Krasheninnikov

University of California at San Diego, La Jolla, CA, USA

I. Introduction. The propagation velocity of intense electron beam in insulator is determined by the velocity of the beam induced ionization wave, which creates enough electrons and ions to neutralize beam charge and current. If the beam density is larger than the electron density that could be provided by ionization, only a fraction of the beam density would be allowed to propagate. Such condition experimentally achieved in experiments on launching a dense electron beam into gas jets [1-3]. Moreover for high beam density the ionization of the insulator is mainly due to the electric field ionization [4-6]. However, the dynamics of secondary electrons in solid insulators and gas jets is very different due to different neutral density and, therefore, collisionality of secondary electrons. In solids we can use drift approximation [6] while in gas jets collisionless ballistic model [7] of secondary electrons has to be used to describe the dynamics of the ionization wave propagation. In this work we generalize the results of [7] on beam propagation through gas jets to the relativistic energies.

II. Equations and numerical solutions. Low density of the gas allows us to neglect collisional ionization and assume that secondary electrons are collisionless. We start with the steady state 1V1D relativistic electron kinetic equation for the secondary electron distribution function $f(x,p)$ in the ionization front frame

$$v(p)\partial f(x,p)/\partial x + e(\partial\varphi/\partial x)\partial f(x,p)/\partial p = S(x,p),\quad S(x,p) = (n_0 - n_i(x))\nu_{EI}(x)\cdot\delta(p-p_f), \qquad (1)$$

where e the elementary charge and p is the electron momentum; φ is the electrostatic potential; S(x,p) is the ionization source, where we assume that the newborn electrons are at rest in the laboratory (gas) frame and, therefore, have momentum $p_f \equiv p(v=-v_f)$ in the moving frame; $\nu_{EI}(x)$ is the field ionization rate; n_0 and n_i are gas and ion densities. The total energy of electron is $\xi(x,p) = (p^2+m^2c^2)^{1/2}c - e\varphi(x)$ and by changing the variables set from (x, p) to (x, ξ) we eliminate the field term in Eq.(1) and find $f(x,\xi) = -\int_x^{x_0} S(x',\xi)/v(x',\xi)dx'$, where x_0 corresponds to the position of the beam head. To find the electron density we need to integrate $f(x,\xi)$ over the momentum space. Using the energy conservation $\xi(x,p) = \xi(x',p')$ we can express the electron momentum p as $p = p(x,\xi(x',p'))$. That allows us to change the integration variable from p to p' to use the δ-function in S

$$n_e(x) = -\int_x^{x_0}\int_0^{\infty}(S(x',\xi)/v(x',\xi))(\partial p/\partial p')dp'dx'. \qquad (2)$$

From $\partial\xi/\partial p = v(x,\xi)$ we have $\partial p/\partial p' = v(x',\xi)/v(x,\xi)$. Using $v = -c/\sqrt{1+(mc/p)^2}$ we find

$$v(x,\xi)\big|_{p'=p_f} = -c\sqrt{1-\left\{\left(1-(v_f/c)^2\right)^{-1/2} + e(\varphi(x')-\varphi(x))/mc^2\right\}^{-2}}, \qquad (3)$$

We can use Eq.(2-3) to find ion density (Z=1) by replacing m with ion mass m_i. The potential term in Eq.(3) becomes (m_i/m) times smaller and can be neglected. Therefore, for ions we have $v(x,\xi)\big|_{p'=p_f} = -v_f$, and Eq.(3) yields the integral equation which has the solution

$$n_i(x) = n_0(1-G(x)), \qquad G(x) = \exp\left(-\int_x^{x_0}\nu_{EI}(x')dx'/v_f\right). \qquad (4)$$

Now we can use Eq.(1-4) to write the final expression for electron density

$$n_e(x) = -n_0\int_x^{x_0}(v_f/v(x,x'))(dG/dx)dx'. \qquad (5)$$

The stationary density of the beam electrons is a function of the potential. The form of the function is determined by the beam energy distribution function. We follow Ref. 6, 7 and use the beam density profile $n_b(\varphi) = \bar{n}_b(e\varphi/W_b)^p$, where W_b is the maximum beam energy in the front frame; $\bar{n}_b$ is the maximum beam density. This profile ensures that the beam has zero density at its head. Since the beam density is an explicit function of the potential φ it is convenient to use the potential φ as the main variable instead of the space coordinate x. Then the Poisson's equation has the form

$$d(E^2/2)/d\varphi = 4\pi e\left\{n_i(\varphi) - n_e(\varphi) - \bar{n}_b(e\varphi/W_b)^p\right\}. \qquad (6)$$

Using the expression for densities in Eq.(4-5) and introducing the dimensionless variables $\psi = e\varphi/W_b$, $\varepsilon = -E/E_a$ and dimensionless parameters $c_f = v_f/c$, $W_c = W_b/mc^2$, $\eta_b = \bar{n}_b/n_0$ we can rewrite Eq.(6) as

$$d(\varepsilon^2/2)/d\psi = P_0\left\{\eta_b\psi^p + \int_0^\psi (1 - 1/V_c(\psi,\psi'))(\partial G/\partial\psi')d\psi'\right\}, \qquad (7)$$

$$V_c(\psi,\psi') \equiv |v|/v_f = \sqrt{1-(1-c_f^2)/(1+[\psi-\psi']\cdot\alpha)^2}\,/c_f, \qquad (8)$$

where $\alpha = W_c\sqrt{1-c_f^2}$, $P_0 \equiv 4\pi W_b n_0/E_a^2$, $E_a = (2/3)(I_a/I_H)^{5/2}e/a_b^2$, $I_H = e^4m/(2\hbar^2)$, $a_b = \hbar^2/e^2m$, $I_H = e^4m/(2\hbar^2)$, and I_a is the gas ionization potential. The effective frequency of the field ionization [8] is $\nu_{EI}(\varepsilon) = \nu_0\exp(-1/\varepsilon)/\varepsilon$, $\nu_0 = 6me^4/\hbar^3$, and

$$G(\psi) = \exp\left\{-(\xi_{bc}/c_f)\int_0^\psi(\nu_{EI}(\varepsilon)/\varepsilon)d\psi'\right\}, \qquad \xi_{bc} = 4.5W_c\sqrt{mc^2/I_H}\,(I_H/I_a)^{5/2}. \qquad (9)$$

The absence of the E-field outside of the ionization wave provides us with two boundary conditions (BCs) for Eq.(7), and to insure that there is no space charge behind the front we impose an additional BC

$$\varepsilon(\psi=0) = \varepsilon(\psi=1) = 0, \qquad d(\varepsilon^2/2)/d\psi\,|_{\psi=1} = 0 \qquad (10)$$

All three BCs for the first order differential equation can be satisfied only by adjusting two free parameters in the equation. We choose these two parameters to be c_f and η_b. We solve Eq.(7-10) numerically for a set gas densities n_0, beam energies W_b, and values of smoothness parameter p. By choosing the appropriate ionization potential we simulate two different gases, Argon and Helium. The calculated values of the front velocity c_f are plotted in Figures 1, 2 as a function of gas density.

First, we recover the simulation results from [7] where it was also noticed that the front is slower for higher ionization potential and for smaller gas density as seen in [2, 3]. Second, the ionization front velocity values measured for Argon and Helium in [2, 3] can be approximately recovered by our model assuming that the beam energy was ~0.5 MeV and p ~ 0.1 (see Figure 1, 2). The beam density predicted by our model is about ~90-99% of the gas density. The agreement with experiment seems to be better for Argon but the number of data points is too small to make a definite conclusion. In the next Sections we analyze Eq.(7-10) and find an approximate expression for front velocity in the limits of small and large velocities.

III. Analysis. Considering the exponential dependence of the field ionization rate on the E-field amplitude, the reasonable assumption to make is that all ionization happens in a narrow region near the maximum value $\varepsilon_I = \varepsilon(\psi_I)$ of the E-field, where the E-field amplitude can be approximated with parabola

$$\varepsilon(\psi \approx \psi_I) \approx \varepsilon_I + \varepsilon_I''(\psi-\psi_I)^2/2, \qquad \varepsilon_I^2 = 2P_0\eta_b\psi_I^{p+1}/(1+p). \qquad (11)$$

where the maximum value of the E-field in the front, ε_I, is estimated from the Poisson's equation where we neglect the induced space charge term (whose integral contribution is small for $\psi < \psi_I$). By substituting Eq.(11) into definition of G in Eq.(9) we find

$$G(\psi_I) \approx \exp\left\{-(1/\Delta\psi_I)\sqrt{-0.5\pi\varepsilon_I^2/\varepsilon_I''}\right\},\ \Delta\psi_I \equiv \left|d\ln G/d\psi\right|_{\psi_I}^{-1} = (c_f/\xi_{bc})(\varepsilon_I/\nu_{EI}(\varepsilon_I)). \qquad (12)$$

Note: due to the assumed symmetry of the E-field around ψ_I (see Eq.(11)) the integral in Eq.(9) will double if we integrate over the whole ionization region instead of just half of it, i.e. $G(1) = G^2(\psi_I)$. From Eq.(12) we find the expression for ε_I'' which can be combined with the expression for ε_I'' found by differentiating Eq.(7)

$$\varepsilon_I'' = (P_0/\varepsilon_I)\left(p\eta_b\psi_I^{p-1} + I_2\right), \qquad I_2 \equiv \int_0^{\psi_I}\{\partial(1-1/V_c(\psi_I,\psi'))/\partial\psi'\}(\partial G/\partial\psi')d\psi'. \qquad (13)$$

If the maximum potential energy gain W_c is much larger than the sum of electron initial kinetic and rest energy, i.e. $\alpha >> 1$, we have from Eq.(8)

$$1/V_c(\psi,\psi') \approx c_f, \qquad I_2 \approx -(1-c_f)G_I/\Delta\psi_I. \qquad (14)$$

Combining two expressions for ε_I we find the thickness of the ionization region $\Delta\psi_I$ and then use Eq.(12) to find c_f

$$\Delta\psi_I \approx (\pi/(1+p))(1-G_I)\varepsilon_I\psi_I/G_I\ln^2 G_I, \quad c_f = (\pi/(1+p))(1-G_I)\xi_{bc}\nu_{EI}(\varepsilon_I)/G_I\ln^2 G_I. \qquad (15)$$

To estimate the values of ψ_I, G_I and ε_I we apply Eq.(7) at $\psi = 1$ and at the point of strongest E-field ψ_I (where $d\varepsilon/d\psi = 0$)

$$\eta_b \approx (1-c_f)(1-G(1)), \qquad \eta_b\psi_I^p \approx (1-c_f)(1-G_I). \qquad (16)$$

We obtain the third equation by integrating Eq.(7) over ψ from 0 to 1 and assuming

$$(\psi_I\varepsilon_I/(1-2\varepsilon_I))(2/(1+p)) << \Delta\psi_I << 1-\psi_I, \quad \eta_b \approx (1-c_f)(1-G(1))(1-\psi_I)(1+p). \qquad (17)$$

The combination of Eq.(16-17) allows us to find the point of strongest E-field $\psi_I = p/(1+p)$. Using $G(1) = G^2(\psi_I)$ we obtain

$$G_I = \psi_I^{-p} - 1, \qquad \eta_b = \psi_I^{-p}(1-c_f)(1-G_I). \qquad (18)$$

Using Eq.(15,18) we find that condition in Eq.(17) is satisfied if p is not too large. In the case of full (or almost full) ionization, G(1)<<1, the better agreement is achieved using the approximation G(1) = 0 which produces $G_I^* = 1-\psi_I^p$, $\eta_b^* = 1-c_f$ (see Figure 3).

Combining Eq.(11,15,18) we can find the equation for ε_I. But this equation has no simple solution and we consider instead two different limits. In the limit $c_f << 1$ we can find ε_I from Eq.(11,18) neglecting c_f compared to 1 and then substitute it into Eq.(15). In the limit $c_f \sim 1$ we can find ε_I from Eq.(15) and then we find c_f from Eq.(11, 18)

$$c_f = 1-(1+p)\varepsilon_I^2/((1-G_I)2\psi_I P_0). \qquad (19)$$

If $\alpha << 1$ it can be shown that if acceleration potential W_c is too small compared to c_f^2, $\alpha << c_f^2/2$, no solution exists. For the intermediate case $c_f^2/2 << \alpha << 1$ we recover Eq.(15), which is equivalent to the result obtained in [6]. Finally, the approximate solutions given in Eq. (15) and Eq.(19) are shown in Figures 1, 2 (curves A_1 and A_2 respectively) together with the corresponding numerical solution.

Here we neglected collisional ionization but it becomes important at small densities when the induced E-field becomes too small compared to atomic field E_a. Using the estimate of the velocity of a pure collisional front $c_f \sim \nu_{ea}\lambda_{Db}/c$ and using Eq.(15) we estimate that collisional ionization become important if $n_b \lesssim W_c^{-1}\cdot 4\cdot 10^{17}\,\mathrm{cm}^{-3}$ (see also Ref. 2). At large beam densities and relativistic velocities the collisional ionization becomes important when

$\nu_{ea}\lambda_{Db}/c \sim 1$ which requires $n_b \gtrsim W_c \cdot 10^{28}\,cm^{-3}$ (that, however, is much larger than density of laser generated beams ~10^{21} cm^{-3}).

IV. Conclusions. The ionization front induced by intensive electron beam in gas was studied in 1D approximation. We generalized the approach developed in [7] to include the relativistic beam energies. We found the approximate expressions for the front velocity and corresponding beam density in the limit of large and small front velocities (see Figure 1-3). We calculated the ionization front velocity in a gas for a wide range of beam energies and gas densities. The calculated front velocity is in a good agreement with the experimental data for Helium and Argon from [2, 3]. More experimental results are needed for comparison. We are planning to use PIC code to further test and improve the model.

Acknowledgements. The work was performed under auspices of the University of Nevada, Reno under grant No. 16BB150784 at UCSD.

References. [1] M. Tatarakis, *et al.*, PRL **90** (2003) 175001; [2] D. Batani, *et al.*, PRL **94** (2005) 055004; [3] M. Manclossi, *et al.*, PRL **96** (2006) 125002; [4] V. T. Tikhonchuk, PoP **9** (2002) 1418; [5] A. J. Kemp, *et al.*, PoP **11** (2004) 5648; A. J. Kemp, *et al.*, PoP **11** (2004) L69; [6] S. I. Krasheninnikov, *et al.*, PoP **12** (2005) 073105; [6] S. I. Krasheninnikov and B. K. Frolov, PoP **13 (**2006**)** 033101; [8] M. V. Ammosov, *et al.*, Sov. JETP **64** (1986) 1191

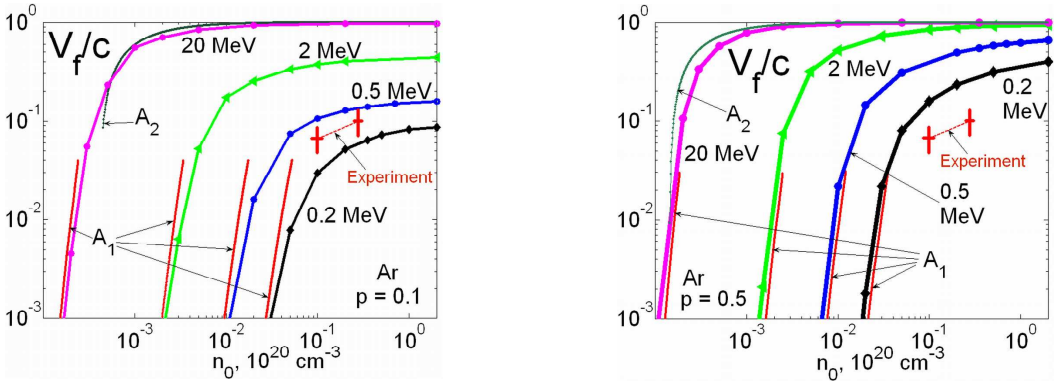

Fig. 1. The front velocity v_f versus gas (Ar) density n_0 for different p and W_b

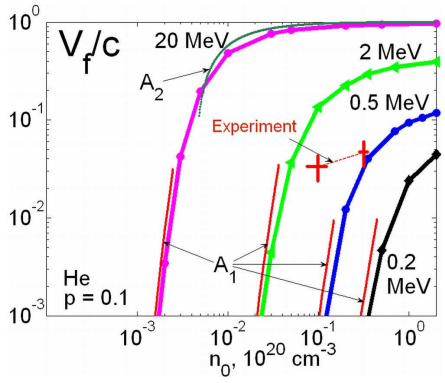

Fig. 2. Same as Fig.1 but for Helium.

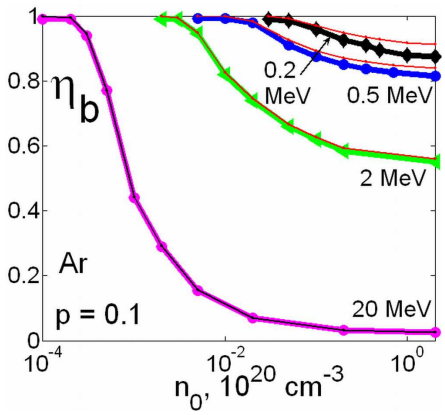

Fig.3. Propagating beam density (red thin curves correspond to $\eta_b^* = 1 - c_f$)